Appendix

Parental Epigenetic Asymmetry of PRC2-Mediated Histone Modifications in the Arabidopsis Endosperm

Jordi Moreno-Romero, Hua Jiang, Juan Santos-González, Claudia Köhler

Table of content

Appendix Figure S1

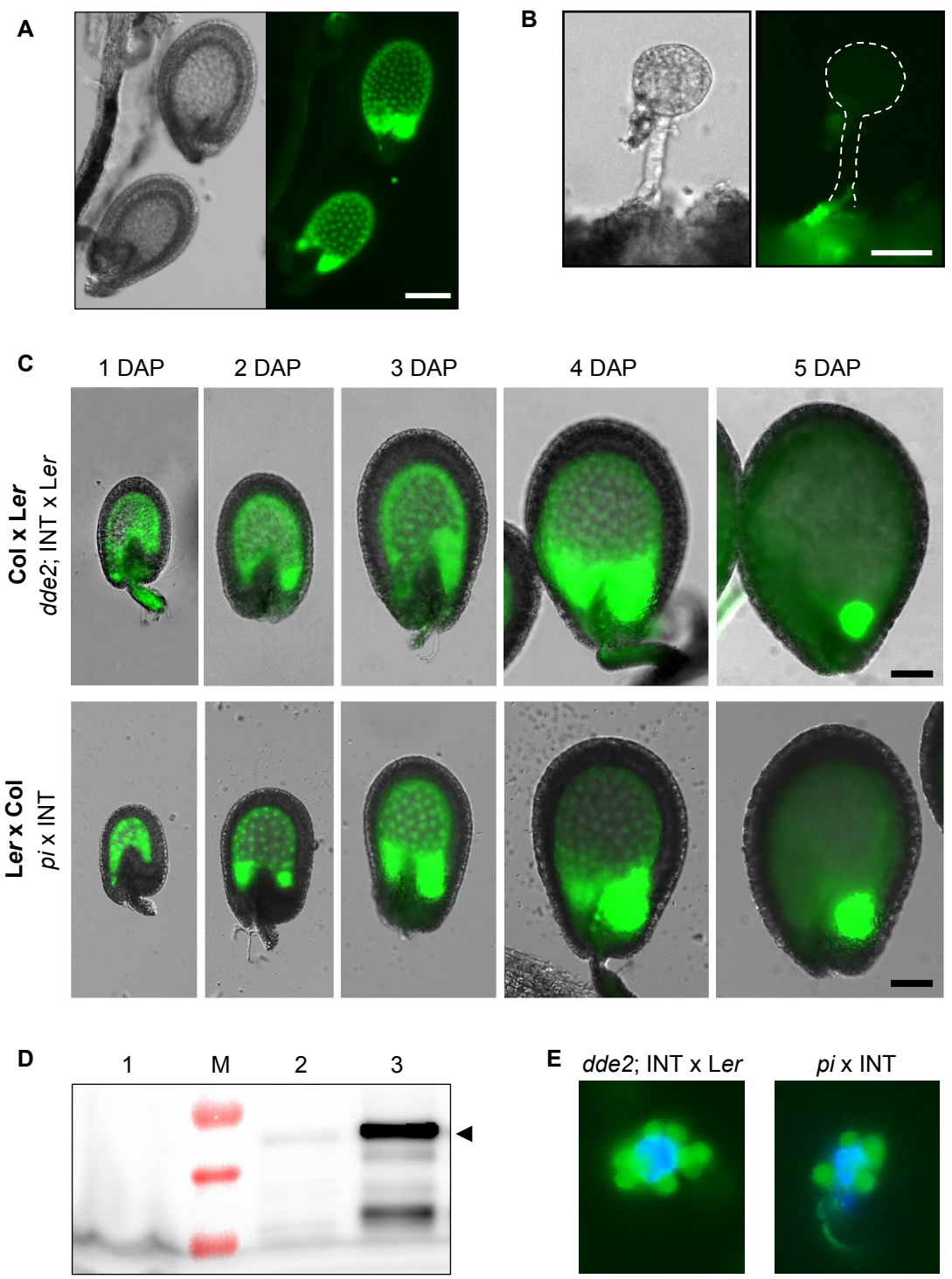

Appendix Figure S2

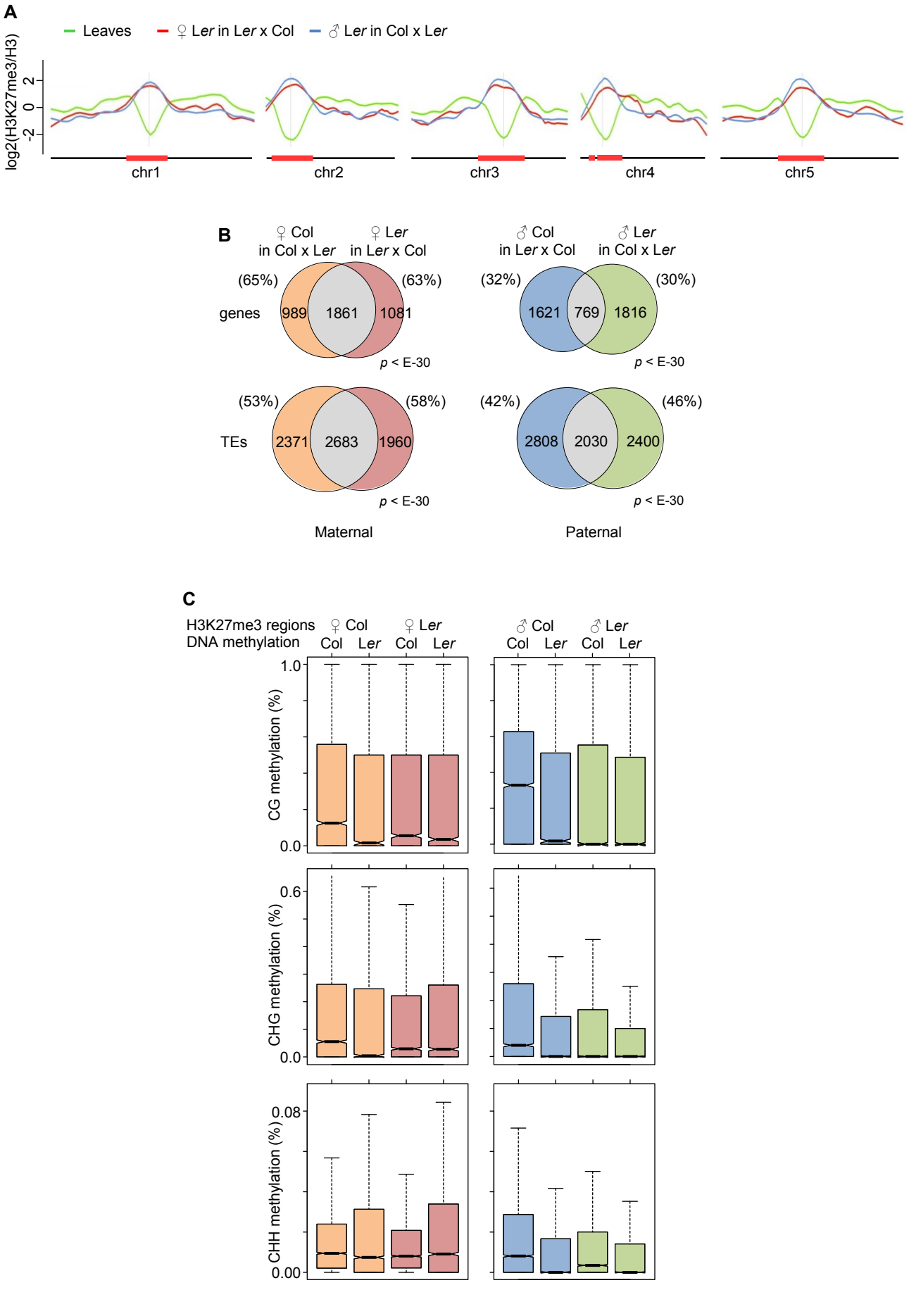

Appendix Figure S3

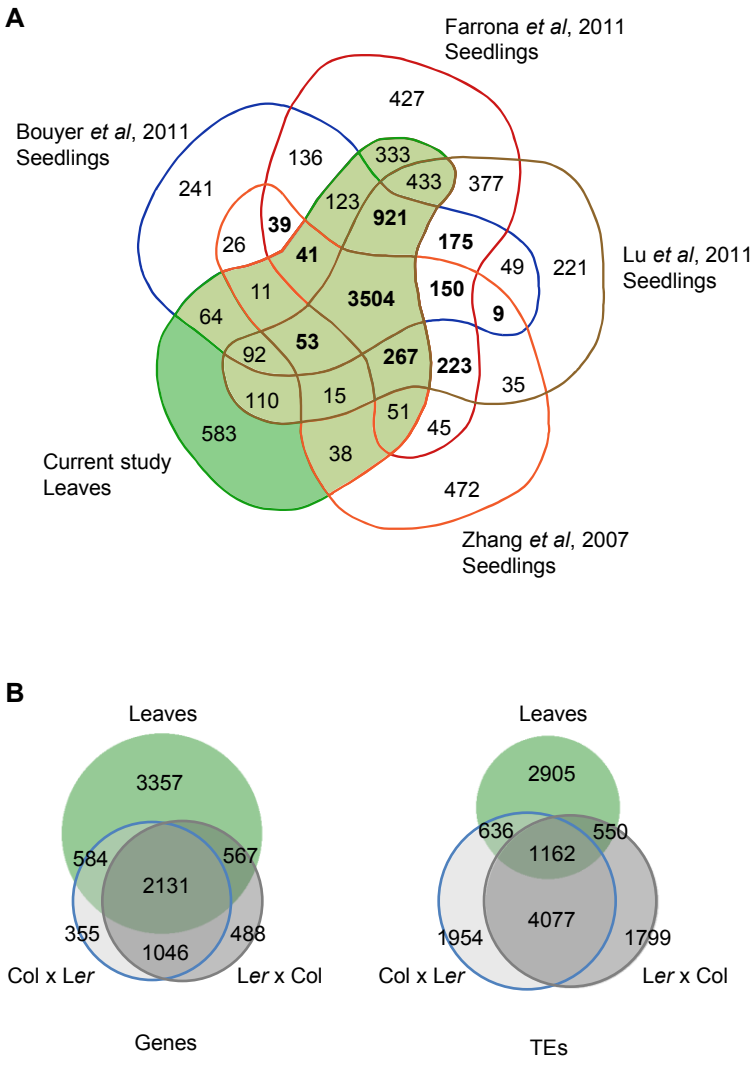

Appendix Figure S4

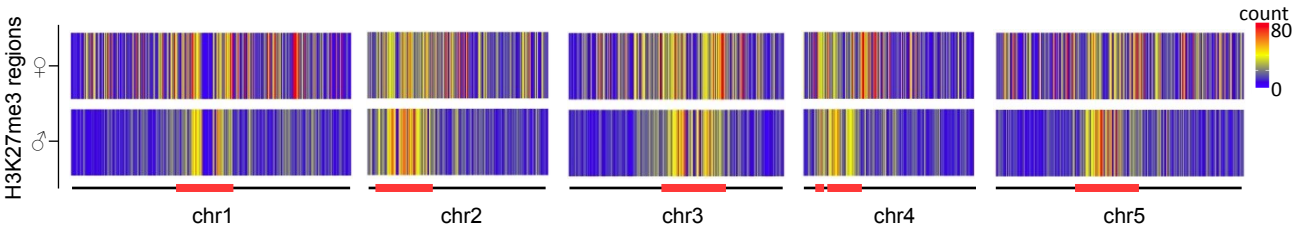

Appendix Figure S5

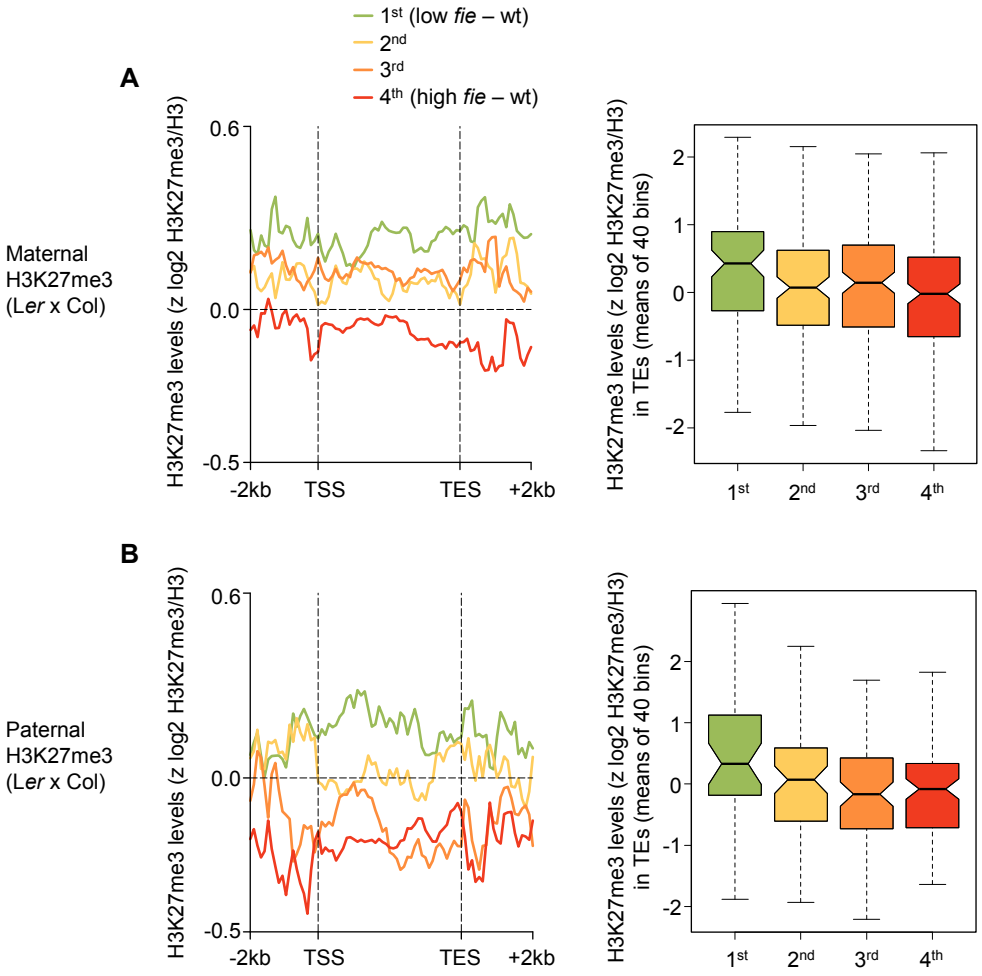

Appendix Figure S6

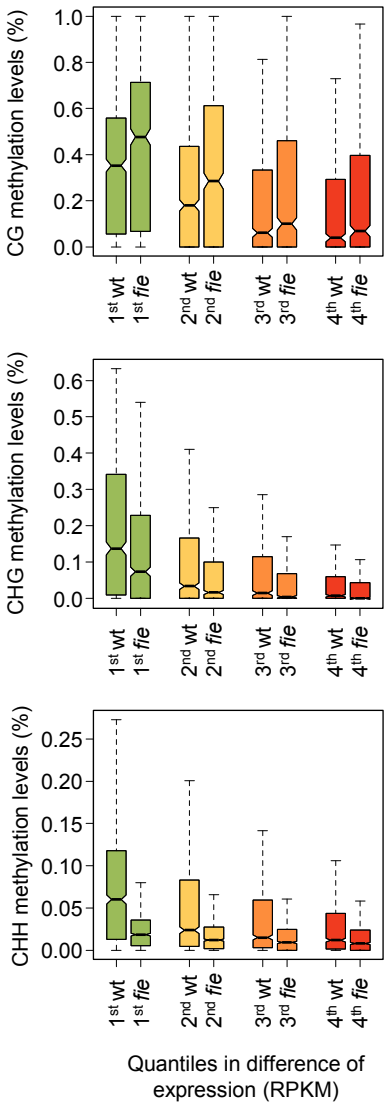

Appendix Figure S7

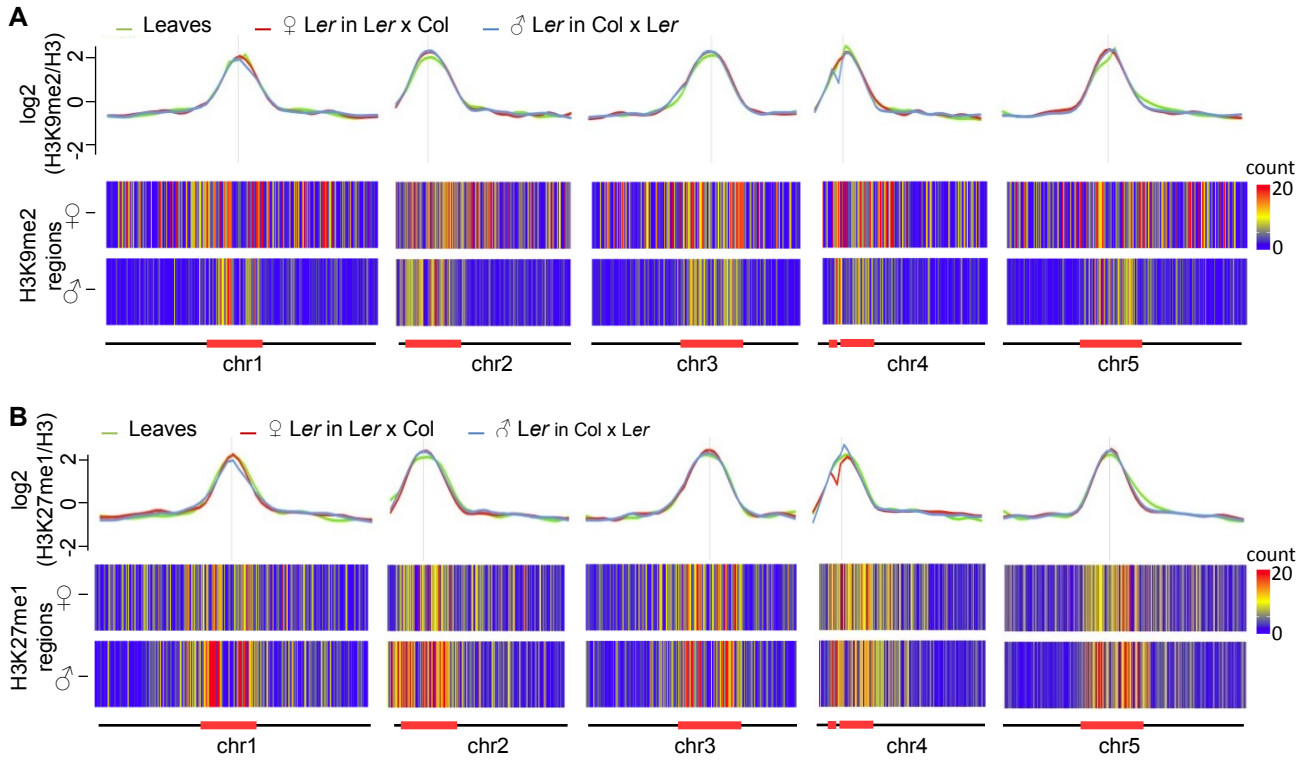

Appendix Figure S8

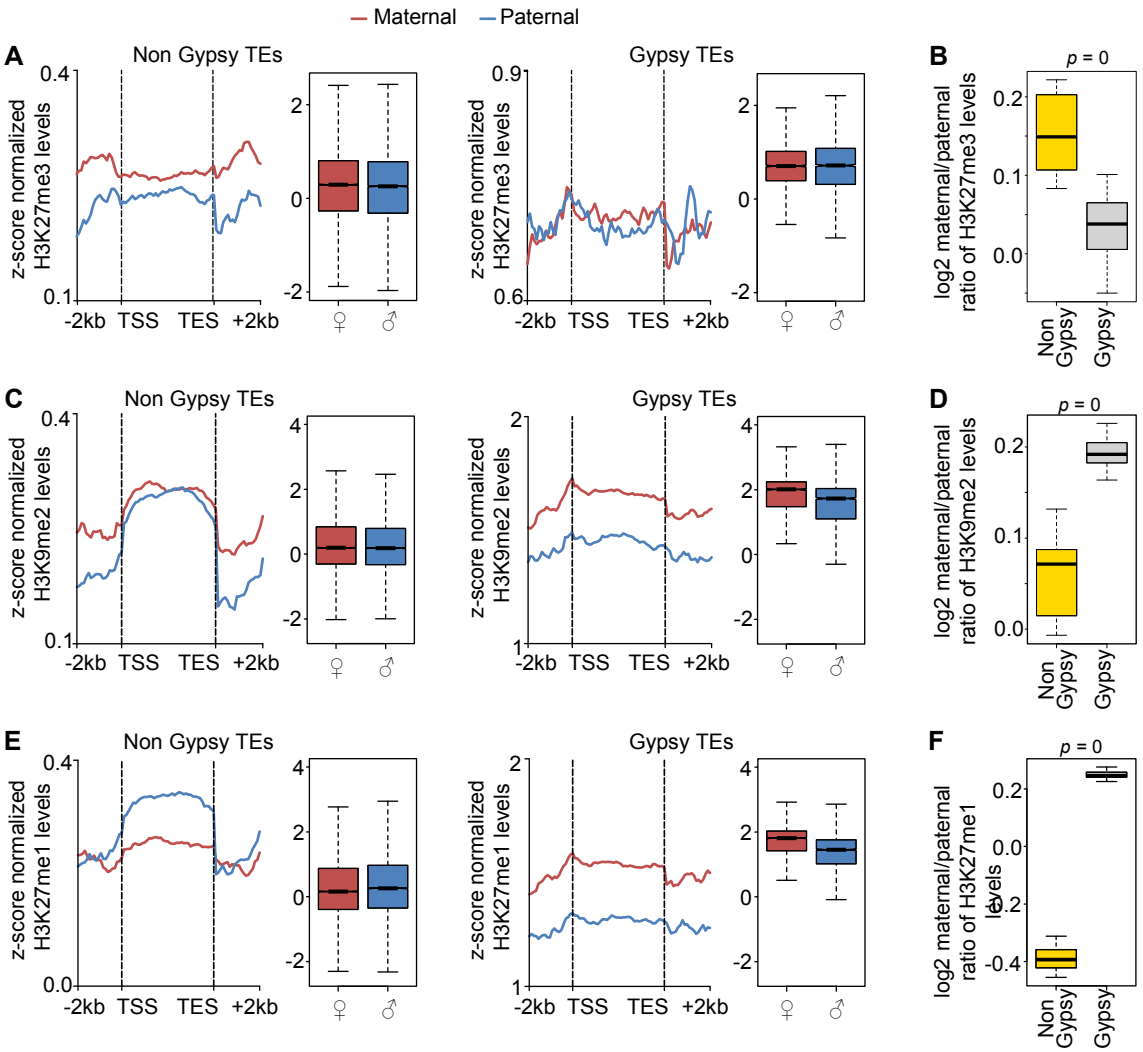

Appendix Figure S9

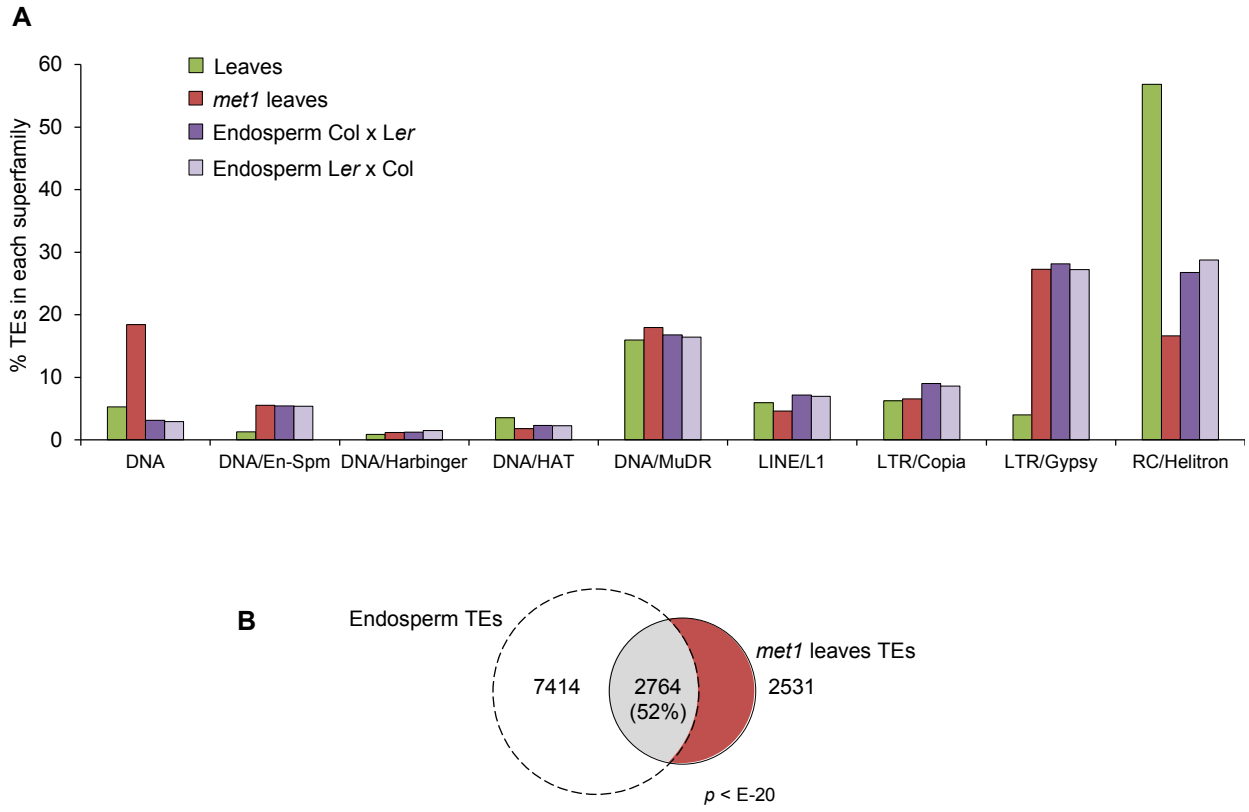

Appendix Figure S10

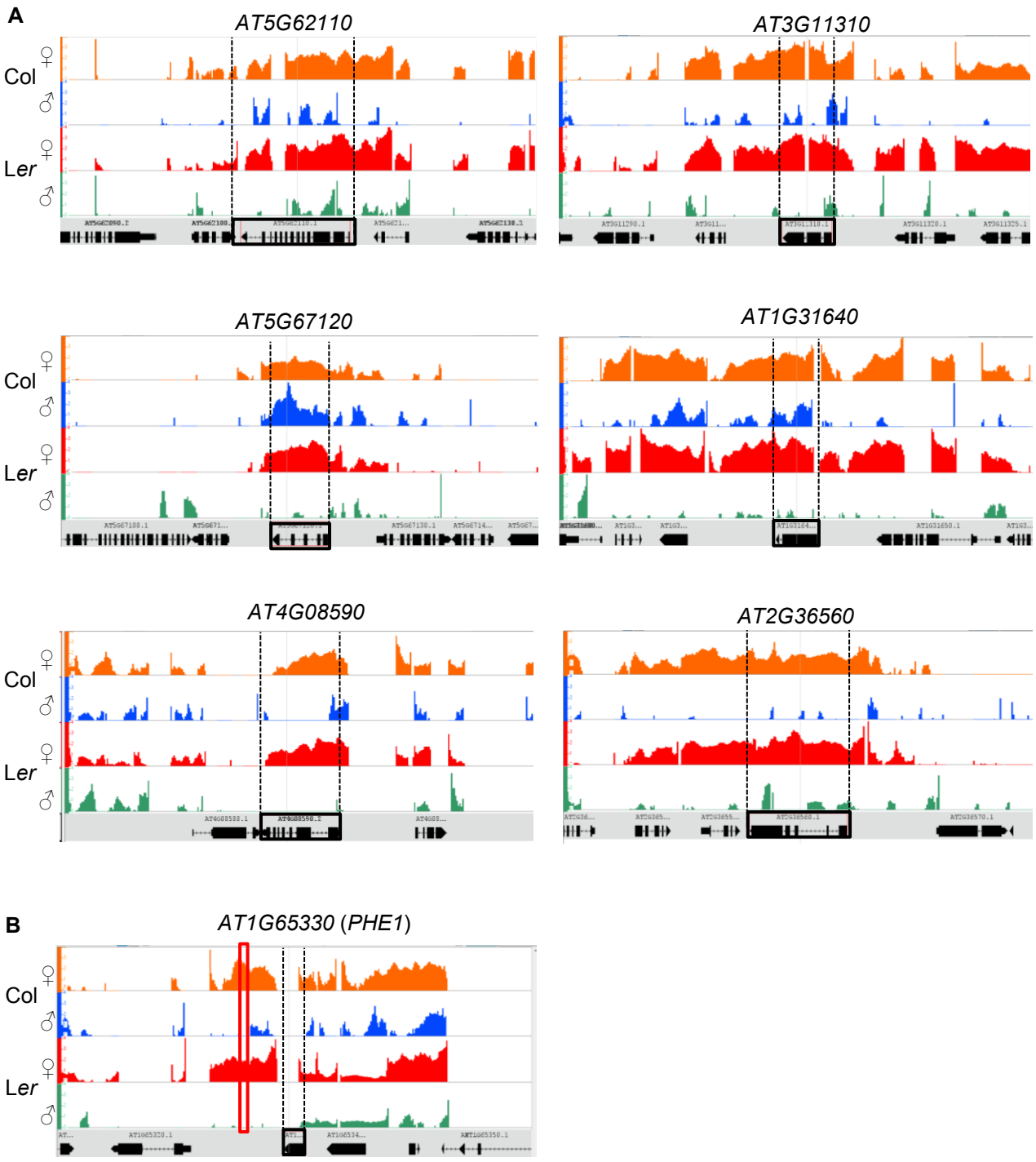

Appendix Figure S11

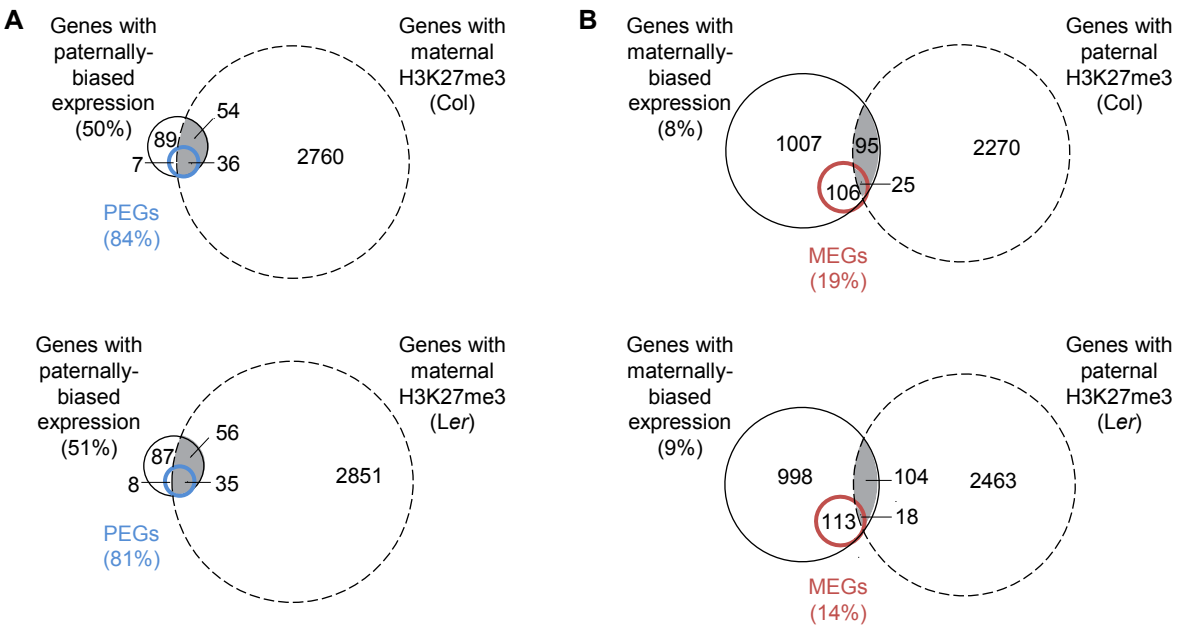

Appendix Figure S12

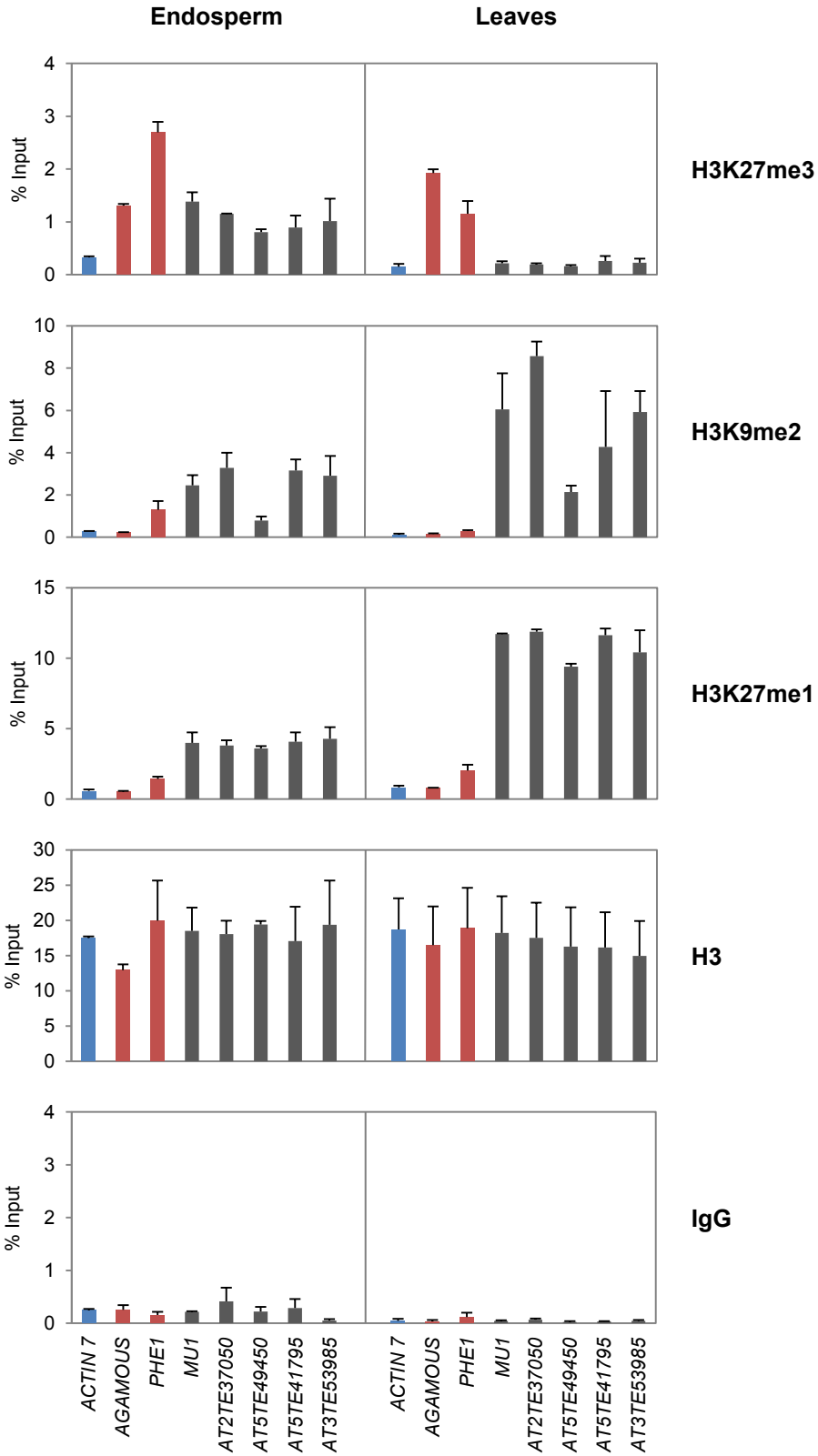

Appendix Figure Legends

Appendix Figure S1. Quality of INTACT (INT) Lines Expressing *NTF* and *BirA* Genes Under Control of the *PHE1* Promoter

A. *PHE1::NTF* is expressed in endosperm nuclei. Pictures are taken at 4 DAP. Scale bar corresponds to 100 μM.

B. *PHE1::NTF* is not expressed in the embryo. Pictures are taken at 4 DAP. Scale bar corresponds to 50 μM.

C. Time course expression analysis of *PHE1::NTF* at 1-5 DAP in seeds derived from crosses of *dde2*; *INT* (in Col) x L*er* (upper panels) and in seeds derived from crosses *pistillata* (*pi*; in L*er*) x *INT* (in Col) (lower panels). Scale bar corresponds to 100 μM.

D. Analysis of *PHE1::BirA* expression by streptavidin antibody western blot. Lanes correspond to: 1- wild type; M- marker: 55, 40 and 35 kDa (corresponding to upper, middle and lower band, respectively); 2- Positive control: *ACT2::NTF; GL2::BirA*; 3- *INT* line. Arrow head indicates the position of the 42-kDa NTF protein.

E. Nuclei binding assay shows binding of nuclei (blue) by the magnetic streptavidin-coated beads (green).

Appendix Figure S2. Parental-Specific Distribution of H3K27me3

A. Chromosomal distribution of z-score normalized H3K27me3 in leaves and on maternal and paternal alleles in the endosperm of the L*er* accession.

B. Accession-specific and shared H3K27me3 genes (upper Venn diagrams) and TEs (lower Venn diagrams) in Col and L*er* accessions. Significance was tested using a hypergeometric test. Numbers in parenthesis correspond to percent of overlap. C. Accession-specific DNA methylation levels at parental-specific H3K27me3 regions as specified in B. Col/L*er* maternal specific regions are regions

only marked by H3K27me3 on the maternal genome in the Col or L*er* accession, respectively. Col/L*er* paternal specific regions are regions only marked by H3K27me3 on the paternal genome in the Col or L*er* accession, respectively. Boxplots represent average levels of parental DNA methylation within H3K27m3 parental specific regions in Col and L*er.*

Appendix Figure S3. Comparison of H3K27me3 Targeted Genes in Leaves and Endosperm

A. Overlap of H3K27me3 enriched genes in leaves identified in this study with previously published datasets. Number of genes present in at least three of the published studies are marked in bold.

B. Overlap of genes (left Venn diagram) and TEs (right Venn diagram) marked by H3K27me3 in leaves and endosperm of Col and L*er* reciprocal crosses.

Appendix Figure S4. Parental-Specific Distribution of H3K9me2 in the *Arabidopsis* Endosperm (L*er*)

Heat map for maternal and paternal specific H3K27me3 distribution in L*er*. Bin size is 100 kbp and colors reflect number of enriched regions.

Appendix Figure S5. Parental-Specific Localization of H3K27me3 on Transposable Elements in the *Arabidopsis* Endosperm

A. Metagene plot of maternal H3K27me3 (left panel) across TEs grouped based on the fold change of expression between *fie* and wild type as in Fig 2D. Box plot (right panel) of expression differences in *fie* and wild type in relation to H3K27me3 levels for the group of TEs shown in the left panel.

B. Metagene plot of paternal H3K27me3 (left panel) across TEs grouped based on the fold change of expression between *fie* and wild type as in Fig 2D. Box plot (right panel) of expression differences in *fie* and wild type in relation to H3K27me3 levels for the group of TEs shown in the left panel.

Appendix Figure S6. DNA Methylation Levels of TEs in *fie*

Box plot of DNA methylation levels in TEs in wild type and *fie* (data from Ibarra *et al* 2012) grouped based on the fold change of expression between *fie* and wild type as in Fig 2D and Appendix Figure S5.

Appendix Figure S7. Parental-Specific Distribution of H3K9me2 and H3K27me1 in the *Arabidopsis* Endosperm

A. Upper panel shows chromosomal distribution of z-score normalized H3K9me2 in leaves and on maternal and paternal alleles in the endosperm of the L*er* accession. Lower panel shows heat map for maternal and paternal specific H3K9me2 distribution in L*er*. Bin size is 100 kbp and colors reflect number of enriched regions.

B. Upper panel shows chromosomal distribution of z-score normalized H3K27me1 in leaves and on maternal and paternal alleles in the endosperm of the L*er* accession. Lower panel shows heat map for maternal and paternal specific H3K27me1 distribution in L*er*. Bin size is 100 kbp and colors reflect number of enriched regions.

C. Average distribution of z-score normalized H3K27me3 levels on maternal and paternal alleles of non-gypsy TE elements (left panel) and gypsy elements (right panel) in the cross Col x L*er*.

D. Box plots showing log2 ratios of H3K27me3 levels on maternal and paternal alleles of non-gypsy and gypsy TE elements in the cross Col x L*er*. Statistical test for difference was done by a Wilcoxon rank sum test.

Appendix Figure S8. Parental-Specific Distribution of H3K27me3, H3K9me2 and H3K27me1 in Gypsy and Non-Gypsy TEs

A, C, E. Metagene plots showing average distribution of z-score normalized H3K27me3 (A), H3K9me2 (C), H3K27me1 (E) levels on maternal and paternal alleles of non-gypsy TE elements (left panel) and

gypsy elements (right panel) in the cross Col x L*er*. Box plots show mean values of z-scored methylation marks shown in the metagene plots.

B, D, F. Box plots showing log2 ratios of H3K27me3 (B), H3K9me2 (D), H3K27me1 (F) levels on maternal and paternal alleles of non-gypsy and gypsy TE elements in the cross Col x L*er*. Statistical test for difference was done by a Wilcoxon rank sum test.

Appendix Figure S9. Redistribution of H3K27me3 to Specific TE Families in the *met1* Mutant

A. Distribution of H3K27me3 marked regions among TE superfamilies in sporophytic tissues of wild-type and *met1* (Deleris *et al*, 2012) and endosperm of Col and L*er* reciprocal crosses.

B. Overlap of TEs that gained H3K27me3 in the *met1* mutant with those marked by H3K27me3 in the endosperm. Significance was tested using a hypergeometric test.

Appendix Figure S10. Parental-Specific H3K27me3 Profiles on Selected MEGs and PEGs in Col and L*er* Accessions

A. Parental-specific H3K27me3 profiles of PEGs *AT5G62110*, *AT3G11310*, *AT5G67120*, *AT1G31640*, *AT4G08590* and *AT2G36560* that are marked by H3K27me3 on the paternal allele but with the exception of *AT5G67120* have higher H3K27me3 levels on the maternal alleles.

B. Parental-specific H3K27me3 profiles at the *PHERES1* (*PHE1*) locus reveal that a differentially methylated repeat region downstream of *PHE1* (Villar *et al*, 2009) is marked by differential H3K27me3 (red box).

The respective genes are marked by black boxes. Black dotted lines mark the 5' and 3' end of the respective genes. Negative H3K27me3 values have been removed.

Appendix Figure S11. Overlap of Genes with Parentally-biased Expression with Genes Marked by H3K27me3

A. Overlap of paternally-biased genes and PEGs with genes marked by H3K27me3 genes on maternal alleles in Col (upper Venn diagram) and L*er* (lower Venn diagram). Paternal bias was estimated using published data (Pignatta *et al*, 2014) by calculating the deviation from the expected ratio of two maternal to one paternal reads by Chi square ($p<0.01$) and an average imprinting score of >2 (Pignatta *et al*, 2014). Numbers in parenthesis correspond to percent of overlap.

B. Overlap of maternally-biased genes and MEGs with genes marked by H3K27me3 genes on paternal alleles in Col (upper Venn diagram) and L*er* (lower Venn diagram). Maternal bias was estimated using published data (Pignatta *et al*, 2014) by calculating the deviation from the expected ratio of two maternal to one paternal reads by Chi square ($p<0.01$) and an average imprinting score of >2 (Pignatta *et al*, 2014). Numbers in parenthesis correspond to percent of overlap.

Appendix Figure S12. ChIP qPCR of genes and TEs in endosperm and leaves

ChIPs from endosperm and leaf tissues were performed using antibodies against H3K27me3, H3K9me2, H3K27me1, H3 and IgG. *ACTIN7* serves as a negative control region for all tested histone modifications. Genes marked by H3K27me3 in the endosperm and leaves (red) and endosperm-specific H3K27me3 targeted TEs (grey) were tested. Error bars represents the s. d. of biological duplicates.